

# An ensemble of Density based Geometric One-Class Classifier and Genetic Algorithm

Do Gyun Kim, Post doctor, rlaehrbs90@ajou.ac.kr

Jin Young Choi\*, Professor, choijy@ajou.ac.kr

Department of Industrial Engineering,  
Ajou University, Korea

## Abstract

One of the most rising issues in recent machine learning research is One-Class Classification which considers data set composed of only one class and outliers. It is more reasonable than traditional Multi-Class Classification in dealing with some problematic data set or special cases. Generally, classification accuracy and interpretability for user are considered as trade-off in OCC methods. Classifier based on Hyper-Rectangle (H-RTGL) is a sort of classifier that can be a remedy for such trade-off and uses H-RTGL formulated by conjunction of geometric rules called interval. This interval can be basis of interpretability since it can be easily understood by user. However, existing H-RTGL based OCC classifiers have limitations that (i) most of them cannot reflect density of target class and (ii) that considering density has primitive interval generation method, and (iii) there exists no systematic procedure for hyperparameter of H-RTGL based OCC classifier, which influences classification performance of classifier. Based on these remarks, we suggest One-Class Hyper-Rectangle Descriptor based on density ( $1 - HRD_d$ ) with more elaborate interval generation method including parametric and nonparametric approaches. In addition, we designed Genetic Algorithm (GA) that consists of chromosome structure and genetic operators for systematic generation of  $1 - HRD_d$  by optimization of hyperparameter. Our work is validated through a numerical experiment using actual data set with comparison of existing OCC algorithms along with other H-RTGL based classifiers.

Keywords: One-Class Classification (OCC), Hyper-Rectangle (H-RTGL), Density, Interpretability, Genetic Algorithm

\*Corresponding author

# 1. Introduction

One-Class Classification (OCC) is considered as one of the most promising issues in machine learning research of recent years. OCC assumes that there exists only one class in data set and all instances not belonging to the class are considered as outliers, which is often confused with binary classification utilizing positive and negative classes (Moya and Hush, 1996). Since both positive and negative class of binary classification are class, however, binary classification is clearly different from OCC assuming only one class. In other words, binary classification is a special case of traditional multi-class classification (MCC). Due to such difference between the number of classes in OCC and MCC, their pattern recognition method for obtaining classifier are different from each other (Hempstalk and Frank, 2008). In case of MCC, purpose of classifier is to distinguish one class from the other and is learned from difference between each class since it is assumed that there exist multiple classes in data set. On the other hand, classifier for OCC aims to describe data set thoroughly and to detect unique feature of target class since it is assumed that there is only one class in data set. In the end, such difference between MCC and OCC results in different learning algorithm for them.

As a result of distinguishing features indicated above, OCC can dominate MCC in data set containing problematic structure. For instance, one can consider imbalanced data set (Sun et al. 2009), which contains exceptionally large or small class causing imbalance among sizes of classes. MCC approaches may show degraded classification performance and computational efficiency since difference among classes can hardly be defined due to their imbalanced size. Data set obtained from manufacturing field can be viewed as an actual example of imbalanced data since defection rate is drastically decreased due to development of technology, which means a class representing defection has very small size. In this situation, OCC can provide more accurate and more efficient performance than MCC by focusing on learning implicit pattern of proper products. Besides, to generate OCC model for class of interest selectively may be more efficient than to generate MCC model considering all classes when big data set consisting of many heterogeneous classes is dealt with (Kang et al. 2015).

Such importance of OCC stimulates an emergence of various algorithms to perform OCC. One approach is Probability-based method that calculates Probability Density Function (PDF) or class probability of target class. Others consider modifications of traditional MCC algorithm such as Support Vector Machine (SVM) and Decision Tree (DT) adjusted for reflecting OCC scheme. However, above-mentioned OCC algorithms have their own limitations (Aggarwal, 2014; Yu, 2005). Precisely, probability-based OCC has selection problem of threshold to discriminate target class and outlier. Even though revised SVM for OCC can guarantee promising classification performance, resulted classifier of it is usually so complex that user cannot understand or interpret the result. This complex classification result brings about difficulty on committing post analysis such as comprehension of internal mechanism of classifier and dataset. On the other hand, modified DT for OCC which can provide classification results clearly understood by user has an ambiguity problem through rule generation procedure. Inefficient artificial or unlabeled data generation may be required due to this feature.

OCC classifier using Hyper-Rectangle (H-RTGL) was suggested to remedy such trade-off between classification accuracy and interpretability (Jeong and Choi, 2015; Kim et al., 2018; Jeong et al., 2019). It determines membership of instances according to H-RTGL surrounding the target class and consisting of geometric rules called interval that can be clearly understood by user, which enables to provide interpretability and maintain prominent classification performance. Various OCC classifiers were defined by different interval generation methods such as merging, partitioning, clustering, Gaussian. Although proposed approaches can deal with the trade-off of traditional OCC classifiers, they have following limitations. Most of proposed classifiers cannot reflect density or distribution of training data, which is essential to explore meaningful and significant pattern of data. For instance, classifiers resulted from interval merging and partitioning depend on individual instances and are prone to overfit

observed instances. That based on clustering shares the same problem since it divides training set by clustering and generates intervals by using the information of cluster directly. Gaussian based H-RTGL (*GbH*) suggested in Kim et al. (2018) can utilize the distribution of training data partially. However, performance of *GbH* was validated in small and simple data set, which means lack of generality. In terms of interval generation method, they used ineffective one-dimensional clustering method for projection points which is essential component for calculating proper interval compromising H-RTGL. Meanwhile, all previous researches tackling H-RTGL based OCC classifier do not proffer any systematic hyperparameter tuning procedure. Since hyperparameters used in OCC classifier using H-RTGL influence the outfit of decision boundary that discriminates target class and outlier, finding proper hyperparameter is an important issue in terms of classification performance. Despite of their importance, hyperparameters are visited by exhaustive and inefficient method such as grid search. In other OCC algorithms such as One-Class 1-SVM, it was proven as meaningful improvement that exploring hyperparameter with optimization method (Liu and Madden, 2007; Tian and Gu, 2010).

Based on mentioned motivation, we intend to get over limitations of existing research by proposing more elaborate H-RTGL based classifier considering density and distribution of target class and dealing with absence of hyperparameter tuning mechanism. We proposed One-Class H-RTGL Descriptor by density ( $1 - HRD_d$ ) and Genetic Algorithm (GA) to generate the new classifier effectively. Suggested classifier can obtain intervals representing target class well by advanced interval generation scheme including both parametric approach which can guarantee optimum split for projection points and non-parametric approaches used to draw prior information for parametric one. Also, designed GA can support classifier generation by optimizing hyperparameters that affects classification accuracy of resulted classifier. We carried out a numerical experiment considering various data set from UCI machine learning repository in order to assess performance of proposed classifier supported by GA.

The rest of this paper is organized as follows. Section 2 contains literature survey summarizing OCC researches proposed as far according to classification methodologies and describing features, pros and cons of each methodology. Then, suggested  $1 - HRD_d$  and GA for systematic generation of classifier are designed in section 3. Proposed algorithm is assessed by numerical experiments in section 4, and we make a remark of our work and suggest further works in section 5.

## 2. Literature survey

We classify existing researches for OCC algorithms as based on classification methodology, namely (i) probability-based OCC, (ii) decision boundary-based OCC, (iii) rule-based OCC, (iv) H-RTGL based OCC. This section explains how each category of algorithm performs OCC and describes detail of proposed literatures.

At first, probability-based OCC can be approximately divided into density estimation and Bayesian approaches. Density estimation approach estimates Probability Density Function (PDF) of given training data set and classifies an instance by calculating probability that the instance belongs to target class according to PDF. Desforges et al. (1998) estimated PDF of positive class in data set by using kernel function and determined instances that had lower probability of PDF than pre-defined threshold as outlier. Ridder et al. (1998) formulated OCC model by using Gaussian and Parzen density estimation and compared classification results to other OCC algorithms. Bishop (1994) dealt with outlier detection of oil flow problem and carried out OCC with Gaussian and Parzen density estimation. Bayesian approach performs OCC by calculating class probability directly with Bayes' theorem under an assumption that features of data set are independent. For example, Datta (1997) proposed Naïve Bayes Positive Class (NBPC) by modifying Naïve Bayes (NB) considering OCC conditions in order to detect only instances of positive class. Denis et al. (2005) applied NB classifier with positive instances reinforced with unlabeled data, and Cohen et al. (2003) committed OCC for facial recognition data set by using Bayesian Network (BN). Such OCC algorithms utilizing probability can classify data intuitively since discrimination can be committed according to probability. However, there is no clear standard for pre-defined threshold used to discriminate between target class and outlier. To overcome this limitation, Hempstalk et al. (2008) considered estimation of class probability as well as density with generating artificial data. Although such approach can alleviate difficulty of threshold selection problem, artificial data cause performance degradation and there is no dominate standard for how many artificial data should be generated. Besides, probability-based OCC algorithms have a weakness in classifying sparse data set since they recognize variation resulted from sparsity as outlier, which hinders suitable classification (Pimental et al., 2014).

Next, decision boundary-based OCC learns pattern of target class in order to obtain a decision boundary which separates feature space into a region including target class and that including outlier. In other words, an instance is determined as target class if it is within the region of target class and as outlier if not. SVM is a representative decision boundary-based classifier used in binary class classification and foundation of OCC methods utilizing decision boundary such as 1-SVM and support vector data description (SVDD). SVDD developed by Tax and Duin (1999, 2004) extracts decision boundary in shape of hyper-sphere including target class in feature space. Especially, it aims to find hyper-sphere which maximizes the number of covered instances belonging to target class and minimizes its radius. Le et al. (2010) introduced concept of margin used by traditional SVM into SVDD and proposed a new objective function of SVDD which maximizes distance between surface of hyper-sphere and outlier. Xiao et al. (2009), Le et al. (2011) suggested multiple SVDD which describes data set by utilizing plural hyper-sphere. 1-SVM proposed by Scholköpfung et al. (2000) performs OCC by finding hyper-plane that separates the origin and target class and maximizes the distance between them. Campbell and Bennett (2001) devised kernel function to linearize complex quadratic programming problem of 1-SVM, Hao (2008) proposed more robust 1-SVM classifier by implementing fuzzy theory. Decision Boundary based OCC can generate classifier with a small sized data set and guarantee outstanding classification performance. However, performance of classifier is highly depending on parameter configuration used to obtain decision boundary. In addition, resulted classifier consists of high-dimensional and complex function which is difficult to interpreted by user.

Rule-based OCC derives some rules that can define an instance as target class from training

data set and classifies new instance according to derived rules. OCC algorithms based on DT and association rule correspond to this category. DT is formulated by rules to classify the instance and proceeds into further depth, until reaching the deepest leaf nodes. Decomite et al. (1999) and Denis et al. (2005) altered C4.5 decision tree which exploits heterogeneity among data to generate rules within decision tree for OCC problem. Two researches formulated decision tree to detect instance of positive class by using positive instances and unlabeled data simultaneously. Lee et al. (1999) considered RIPPER algorithm which enables decision tree to be simplified by using pruning and carried out OCC with fewer rules. Association rule refers serial rules occurred in data set, and common rules to define the instance of target class in classification problem. Brause et al. (1999) extracted association rule from credit information by using neural network in order to prevent credit fraud. Tandon and Chan (2007) compared effect of weighting and pruning occurring in the extraction process of association rules for OCC. OCC methods belonging to this category can provide classification results that can be easily understood and analyzed by user since classifier consists of explicit rules. However, these methods cannot obtain structural classifier since they are prone to overfitted into training data and computational complexity grows drastically as the number of features increases.

H-RTGL based OCC considered in this paper is OCC method that combines features of decision boundary based and rule-based OCC. It extracts decision boundary that has a shape of H-RTGL, which is formulated by conjunction of intervals obtained from each feature. Such decision boundary can be clearly understood by user while that of SVDD or 1-SVM is hard to interpret. Classifier belonging to this group can be categorized according to interval generation method. One-Class H-RTGL Descriptor based on merging ( $1 - HRD_m$ ) draws many small intervals from all instances belonging to target class and finalize conjoint interval set by merging overlapped intervals, whereas One-Class H-RTGL Descriptor based on partitioning ( $1 - HRD_p$ ) obtains conjoint interval set by partitioning one large interval including all instance of target class (Jeong and Choi, 2015; Jeong et al., 2019). These approaches can generate too many H-RTGLs depending on used data set, which results on classifier ignoring distribution or density of data set. *GbH* can handle mentioned restrictions by considering density and distribution of data in interval generation procedure (Kim et al., 2018). However, *GbH* has also limitation that it assumes the same number of distribution and *k*-means clustering used as one-dimensional clustering method may fall into local optimum.

### 3. Design of a new classifier

#### 3.1. OCC definition and classification idea

In general, OCC problem is to determine whether an instance belongs to target class or not when given data set is containing only one class. We use following notations to define such problem. We consider a data set  $X = \{x_1, x_2, \dots, x_n\}$  including  $n$  instances. An instance  $x_i$  contains  $q$  features and can be represented as  $x_i = (y_{i1}, y_{i2}, \dots, y_{iq})$ , where  $y_{ir}$   $r$ -th feature of instance  $x_i$ . The objective of this problem is to formulate a classifier to distinguish instance belonging to target class from outlier. Meanwhile, H-RTGL based OCC is a sort of solution approach to solve this problem and it formulates classifier by committing 3 steps namely i) interval generation, ii) interval conjunction, iii) classifier acquisition, which can be described as [Figure 1]. Since interval is generated feature by feature manner, instances of training data should be projected into each feature. Intervals are obtained from projection points of each feature considering various interval generation methods such as merging and partitioning. Then, prototype of H-RTGL is derived by conjunction of intervals resulted from cartesian product and volume of the H-RTGL is adjusted to prevent overfitting. Finalized H-RTGL is used as classifier to discriminate target class and outlier.

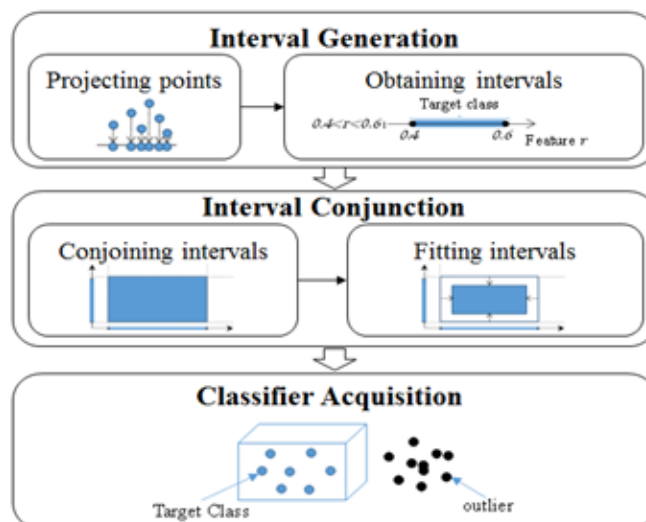


Figure 1. Procedure of 1 – HRD

In this paper, we suggest One-Class H-RTGL Descriptor based on density ( $1 - HRD_d$ ) which generates interval by considering density of projection points represented by statistics of Gaussian distribution. Specifically, we commit clustering into a set of projection points and assign Gaussian distribution for each cluster under assumption that projection points are originated from a certain Mixture of Gaussians (MoG). Intervals are calculated from statistics of Gaussian distribution corresponding to each cluster of projection points. In such interval generation scheme, shape of interval depends on the number of Gaussian distributions and clustering method for projection points. To determine proper number of Gaussian distributions, we apply Kernel Density Estimation (KDE) used to indicate PDF of data set, which enables to estimate approximate shape of the MoG expected to generate projection points (Parzen, 1962). Then, the number of Gaussian distributions  $Ng_r$  used in feature  $r$  is found from resulted PDF. In terms of clustering method for projection points, we consider Jenks natural breaks optimization (Jenks) which is specialized for one-dimensional clustering and can explore optimal solution by enumeration (Jenks, 1967). As a result, systematic interval generation can be committed by choosing proper number of Gaussian distributions  $Ng_r$  and obtaining meaningful cluster of projection points, which can be basis of H-RTGL based classifier with high performance.

### 3.2. Detailed classifier acquirement process of $1 - HRD_d$

Interval generation of  $1 - HRD_d$  is committed feature by feature. Therefore, instances belonging to training data should be projected into each feature prior to interval generation. We define a projection function which projects instance  $x_i$  into feature  $r$  as

$$proj_r(x_i) = y_{ir}, \forall i. \quad (1)$$

[Figure 2] portrays the projection function applied in feature space.

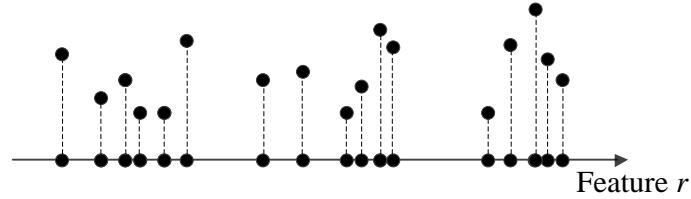


**Figure 2. Projection of instances into feature  $r$**

After a set of projection points in feature  $r$  is obtained, the set is divided into some clusters corresponding to Gaussian distributions. At first, we carry out KDE which estimates density of sample data set in non-parametrical manner by using kernel function. PDF of feature  $x$   $\hat{f}_h$  resulted from KDE is calculated by summation of kernel function  $K$  generated from instance  $x_i$ , which is described as

$$\hat{f}_h(x) = \frac{1}{nh} \sum_{i=1}^n K\left(\frac{x - x_i}{h}\right), \quad (2)$$

where  $n$  is the number of observed instance and  $h$  is bandwidth of kernel function  $K$ . Thus, the shape of estimated PDF depends on kernel function  $K$  and its bandwidth  $h$ . [Figure 3] illustrates variation on the shape of PDF affected by (a) different kernel function and (b) different bandwidth.

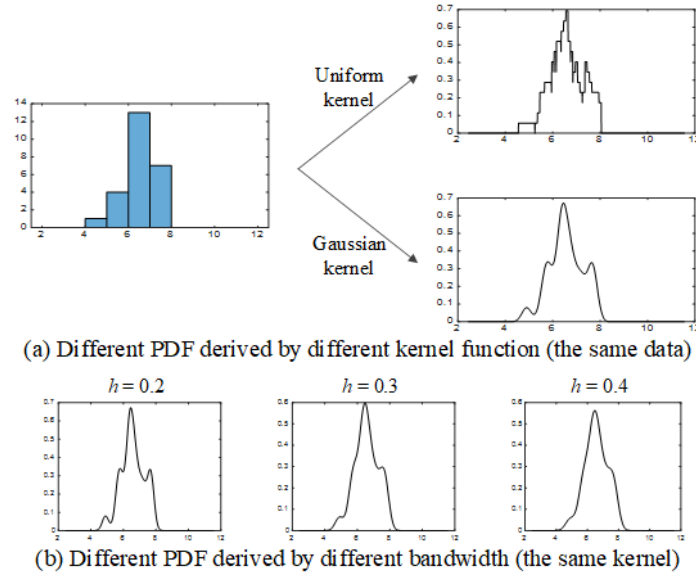


**Figure 3. Effects on PDF of different kernel function and bandwidth**

To derive the number of Gaussian distributions  $Ng_r$  used in feature  $r$ , we consider the number of extreme points appearing in estimated PDF under assumption that presence of one extreme point denotes presence of one Gaussian distribution in MoG. Then, the number of Gaussian distributions  $Ng_r$  varies with kernel function  $K$  and its bandwidth  $h_r$  used in feature  $r$ , which means they are

crucial hyperparameter used for interval generation procedure occurring in feature  $r$  since length and shape of interval depends on  $Ng_r$ . We adopt Gaussian kernel function by assessing both efficiency and effectiveness, and detailed result will be written in section 4. In terms of bandwidth of kernel function, we design Genetic Algorithm (GA) to explore an optimal bandwidth of kernel function  $h_r$  which optimize classification performance of resulted classifier and detailed design of GA will be described in subsection 3.2.

After the number of Gaussian distributions  $Ng_r$  used in feature  $r$  is determined, we commit one-dimensional clustering on projection points by using  $Ng_r$  as a parameter for Jenks. Jenks is clustering method which finds clusters minimizing sum of inter-variability between clusters and intra-variability within clusters. It can avoid converging to local optimum by providing all possible variance information resulted from clusters, which enables Jenks to dominate  $k$ -means clustering. Detailed procedure of Jenks is as follows (Jenks, 1977).

Step 1) Calculate Sum of squared deviations for array mean (SDAM), which can be expressed as equation (3).

$$SDAM = \sum_{i=1}^n (x_i - \mu)^2 \quad (3)$$

Step 2) Enumerate possible class combination and calculate Sum of squared deviations for class means (SDCM) in each resulted class cases, which can be expressed as equation (4).

$$SDCM_c = \sum_{x_i \in c} (x_i - \mu_c)^2 \quad (4)$$

Step 3) Evaluate Goodness of Variance Fit (GVF) calculated from each class combination, which can be expressed as equation (5).

$$GVF = \frac{SDAM - \sum_c SDCM_c}{SDAM} \quad (5)$$

Step 4) Choose the class configuration with greatest GVF.

As a result of one-dimensional clustering,  $Ng_r$  clusters of projection point are obtained. To generate intervals by using them, Gaussian distribution is assigned in each cluster with an assumption that projection points belonging to cluster follow the distribution. Gaussian distribution  $G_r^{q_r} \sim N(\mu_r^{q_r}, \sigma_r^{q_r})$  corresponding to  $q_r$  ( $q_r = 1, 2, \dots, Ng_r$ )-th cluster of projection points in feature  $r$  has mean  $\mu_r^{q_r}$  and standard variation  $\sigma_r^{q_r}$  calculated from cluster of projection points  $C_r^{q_r}$ . An interval of  $1 - HRD_d$  is generated by considering these statistics and the interval corresponding to  $G_r^{q_r}$  is calculated as follows, where  $N_\sigma$  is a parameter to control the degree of influence of  $\sigma_r^{q_r}$  and is optimized by pre-test.

$$ITVL_r^{q_r} = [\mu_r^{q_r} - N_\sigma \sigma_r^{q_r}, \mu_r^{q_r} + N_\sigma \sigma_r^{q_r}] \quad (6)$$

For example, [Figure 6] describes a calculation example of intervals used in  $1 - HRD_d$ . If  $Ng_r$  is determined to 3, three Gaussian distributions can be assumed for three clusters of projection points such as [Figure 4-(a)] and resulted intervals from each distribution are depicted as [Figure 4-(b)]. Since projection points are clustered in  $Ng_r$  clusters in each feature  $r$  and  $q$  features are given in

entire data set, the total number of intervals is calculated as  $\sum_{r=1}^q Ng_r$ .

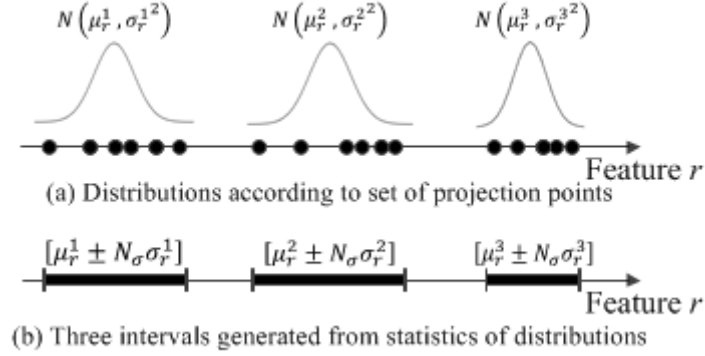


**Figure 4. Deriving intervals from distributions**

Formulation of H-RTGL is committed by conjunction of resulted intervals generated feature by feature. This conjunction of intervals is derived by  $q$ -fold Cartesian product operation and total number of possible interval conjunctions is  $\prod_{r=1}^q Ng_r$  theoretically. Nevertheless, considering all these interval conjunctions deteriorates computational efficiency and has a risk such that a meaningless interval conjunction is generated, or outliers are included in that conjunction. Thus, we use interval conjunction including any instance of training data set and the interval conjunction  $\pi(q_1, q_2, \dots, q_q)$  is described as

$$\pi(q_1, q_2, \dots, q_q) = \prod_{r=1}^q ITVL_r^{q_r} = ITVL_1^{q_1} \times ITVL_2^{q_2} \times \dots \times ITVL_q^{q_q}. \quad (7)$$

If the number of Gaussian distributions  $Ng_r$  used in feature  $r$  is given (2,2) in data set with  $q = 2$ , there are 4 possible interval conjunction. However, we only use interval conjunctions  $\pi(1,1)$  and  $\pi(2,2)$  including instance of training data and ignore other regions, which is depicted as [Figure 5].

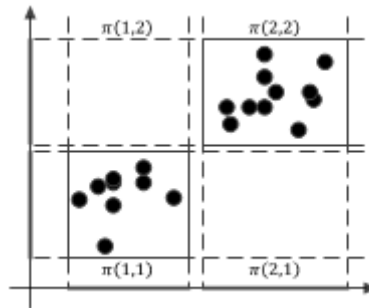


**Figure 5. Example of interval conjunction considering instances**

Even if interval conjunctions filtered by existence of instance can be viewed as H-RTGL and provide efficiency and accuracy, these interval conjunctions have still a risk of overfitting since their intervals are generated feature by feature. To alleviate the risk of overfitting, additional fitting procedure of H-RTGL is required. We propose following 3 fitting functions to control size of H-RTGL and classification results of each fitting function are recorded respectively in numerical experiments so that they can be compared to each other. Commonly used parameter  $v_r$  is used to control volume of H-RTGL.

Fit 1) Instance based fitting : It controls interval by using the minimum and maximum value of instances in interval conjunction, where  $x_j$  is the  $j$ -th projection point included in  $ITVL_r^{q_r}$ .

$$Fit_r(\pi(q_1, q_2, \dots, q_q)) = \left[ \min_{x_j \in ITVL_r^{q_r}} proj_r(x_j) - v_r, \max_{x_j \in ITVL_r^{q_r}} proj_r(x_j) + v_r \right], \forall r \quad (8)$$

Fit 2) No fitting : It uses generated interval without any modification.

$$Fit_r(\pi(q_1, q_2, \dots, q_q)) = [\min(ITVL_r^{q_r}) - v_r, \max(ITVL_r^{q_r}) + v_r], \forall r \quad (9)$$

Fit 3) Density based fitting : It controls interval by using density of instances within interval conjunction.  $proj\_density_r$  is relative density of projection points into feature  $r$  and belonging to interval conjunction  $\pi(q_1, q_2, \dots, q_q)$ . If density of projection points within the interval is greater than or equal to  $1/Ng_r$ , the interval length is increased and otherwise the interval becomes narrow.

$$Fit_r(\pi(q_1, q_2, \dots, q_q)) = proj\_density_r [\min(ITVL_r^{q_r}) - v_r, \max(ITVL_r^{q_r})] + v_r, \forall r \quad (10)$$

In the end, H-RTGL is finalized by logical product operation of intervals adjusted with fitting functions and they are used to determine membership of an instance. Specifically, such H-RTGL is named as Density based H-RTGL (*DbH*) and the instance is considered as target class whether it is in *DbH* or not.

### 3.3. Genetic Algorithm (GA) for efficient selection of Hyperparameter

In addition to suggest  $1 - HRD_d$  which enables to generate promising classifier considering density and distributions of dataset, we design Genetic Algorithm (GA) to choose proper hyperparameter influencing performance of it. Specifically, bandwidth of kernel function  $h_r$  in feature  $r$  is essential hyperparameter since it determines the shape of PDF estimated by KDE and the number of Gaussian distributions  $Ng_r$  used in interval generation of  $1 - HRD_d$ . Therefore, an objective of the designed GA is exploring optimal combination of  $h_r$  in all features which maximizes classification performance of  $1 - HRD_d$ . The entire process of GA is summarized as [Figure 6] and detailed description of the algorithm is written in following subsections.

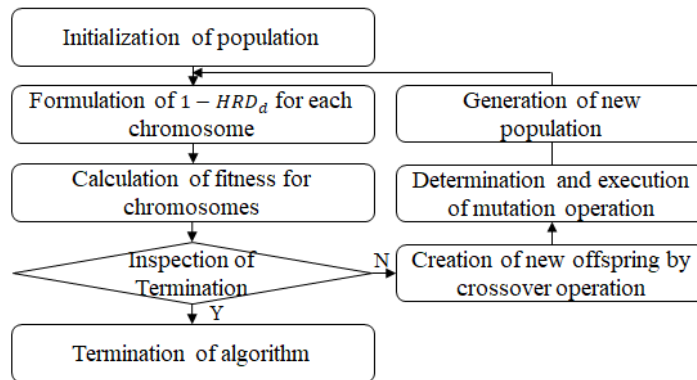


Figure 6. Flowchart of GA

### 3.2.1 Representation of chromosome structure and initial population

To define expression scheme of chromosome composing population is the most prior step which should be considered for design of GA. Considering the objective of GA, we devise a chromosome structure using real-valued encoding scheme and consisting of genes corresponding to each feature in order to record bandwidth of kernel function  $h_r$  in each feature. Since there exist  $q$  features in the data set, a chromosome is defined as a vector with size  $q$  and chromosome structure can be depicted as [Figure 7].

$$h_r: \begin{array}{|c|c|c|c|c|} \hline 0.5 & 1.0 & 0.3 & 1.1 & 1.0 \\ \hline \end{array}$$

**Figure 7 Chromosome structure using real-valued encoding scheme**

Size of Population used in GA is defined as  $P$  and initial population is generated by randomly considering an upper bound  $UB_r$  and lower bound  $LB_r$  used in feature  $r$ . The upper and lower bound  $UB_r$  and  $LB_r$  are calculated as follows. Equation (11) expresses Silverman's rule-of-thumb bandwidth estimator for minimizing Mean Squared Error (MSE), where  $h^*$  is an optimal bandwidth,  $\hat{\sigma}$  is standard deviation of sample and  $n$  express sample size respectively (Silverman, 1986).

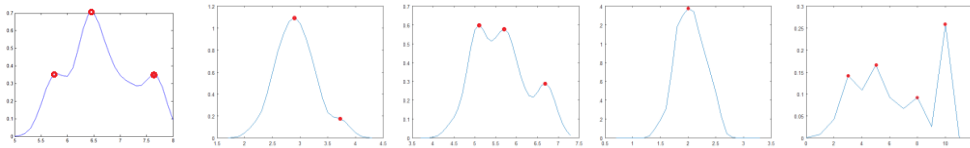
$$h = 1.06\hat{\sigma}n \quad (11)$$

Although  $h^*$  calculated from the equation can minimize MSE for KDE, it cannot guarantee optimality for classification performance of  $1 - HRD_d$  resulted from itself, which is proven by a numerical experiment. Therefore, we set the upper and lower bound  $UB_r$  and  $LB_r$  as a multiplier of  $h^*$  in order to utilize partial information of projection points in each feature.

The chromosome containing bandwidth of kernel function  $h_r$  for each feature  $r$  is decoded by using KDE in order to obtain the number of Gaussian distributions  $Ng_r$  used as crucial parameter of Jenks. [Figure 8] depicts this process of decoding, which includes (a) KDE using  $h_r$  recorded in the chromosome, (b) finding extreme points from PDF estimated by KDE, (c) resulted number of Gaussian distributions  $Ng_r$ .

$$h_r: \begin{array}{|c|c|c|c|c|} \hline 0.5 & 1.0 & 0.3 & 1.1 & 1.0 \\ \hline \end{array}$$

(a) Chromosome describing bandwidth  $h_r$



(b) PDF obtained from KDE using  $h_r$  and extreme points(marked)

$$Ng_r: \begin{array}{|c|c|c|c|c|} \hline 3 & 2 & 3 & 1 & 4 \\ \hline \end{array}$$

(c) The number of distribution used in feature  $r$

**Figure 8 Decoding procedure of a chromosome to obtain the number of distributions**

### 3.2.2 Fitness function

GA performs iterative searching process to enhance solution by transferring good solutions containing desirable features to offspring. To achieve this purpose, a user defines fitness function proper criteria to evaluate chromosomes in population. Since main object of GA proposed in this paper is

solving OCC problem by generation of  $1 - HRD_d$ , fitness function should be capable of evaluating chromosomes according to classification performance obtained by using them. Therefore, we define following fitness function proportional to  $AUC$ , where  $AUC$  is Area Under ROC Curve (AUC) which is one of a measure to assess classification performance and will be explained in section 4 and  $c$  is a constant.

$$fitness\_function = \frac{1}{c} AUC \quad (12)$$

### 3.2.3 Crossover operator

An offspring is generated by inheriting various features from parents in natural evolutionary process. GA imitating this process has also crossover operator to generate the offspring by considering features of parental chromosome. One of the most common crossover operators is one or point crossover, which exchanges genes of parental chromosome according to randomly selected crossover point. However, such point crossover is not suitable for chromosome structure considered in this paper, which contains genes representing the bandwidth  $h_r$  of KDE used in feature  $r$  and arranged feature by feature. Instead, we use arithmetical crossover operator which can generate offspring by arithmetic operation among values recorded in parental chromosome. Particularly, two gene values  $y_r^1$  and  $y_r^2$  of an offspring in feature  $r$  are calculated from  $x_r^1$  and  $x_r^2$  recorded in parental chromosome. [Figure 9] depicts (a) concept of arithmetic crossover and (b) an example of offspring generation using it, where  $\alpha$  is a random number between -0.5 and 1.5 which is used for crossover operation.

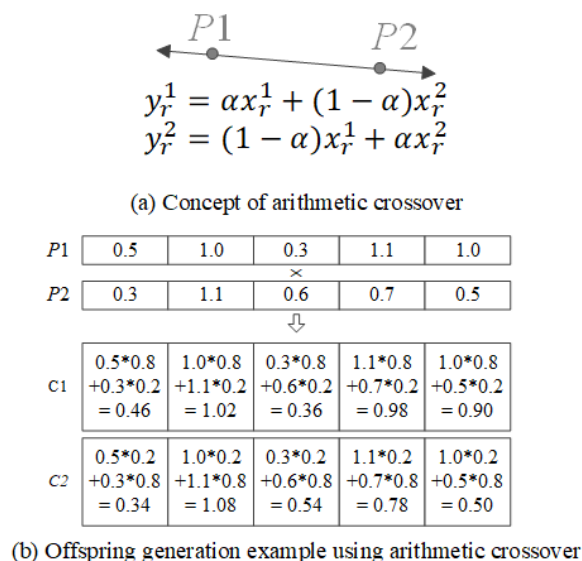


**Figure 9. Concept and example of arithmetic crossover**

### 3.2.5 Mutation operator

In reproduction process of evolution occurring in nature, an offspring generated from crossover operation may contain completely different feature not appearing in parents. This unexpected alteration is called mutation and this new feature triggered by mutation is foundation for diversity of species, which is essential for evolutionary process. Similarly, GA has a mutation operator that mimics mutation in nature and diversity of solutions guaranteed by mutation operator prevents solutions from converging to local optimum. We adopt Makinen, Periaux and Toivanen Mutation (MPTM) operator

that can maintain scalability and efficiently search solution space in real-valued encoding (Makinen et al. 1999, Deep and Thakur, 2007). Detailed procedure to calculate bandwidth  $h'_r$  affected by MPTM operator is as follows.  $UB_r$  and  $LB_r$  are the same as values used to generate initial population.

Step 1) Calculate  $t = (h_r - LB_r)/(UB_r - LB_r)$ .

Step 2) Generate random number  $rnd = [0,1]$ , and compute  $t'$  as follows.

$$t' = \begin{cases} t - t \left( \frac{t - rnd}{t} \right), & rnd < t \\ t, & rnd = t \\ t + (1 - t) \left( \frac{rnd - t}{1 - t} \right), & rnd > t \end{cases}$$

Step 3) Set  $h'_r = (1 - t')LB_r + t'UB_r$ .

### 3.2.5 Population update and termination condition of GA

Through crossover and mutation operator, new generation consisting of  $P$  chromosomes is produced and there exist total  $2P$  chromosomes. To maintain the size of population, we assess fitness value of whole population and select only  $P$  chromosomes with high fitness value. For selection of parental chromosome used to generate next generation, we perform roulette wheel selection based on fitness value. In other words, a chromosome is chosen as parental chromosome by probability which is proportional to its fitness value. Solution space can be explored efficiently due to this selection policy. Besides, GA requires termination criteria to stop the algorithm since there may be only little enhancement after plenty of iterations are performed, which means additional executions are insignificant or not promising. For instance, GA terminates if pre-defined number of iterations or certain computing power allocated is reached. However, we adopt termination condition if there is no enhancement after a certain number of generation (5 in this paper), since this termination condition can enable more exhaustive and efficient searching for solution space than other criteria (Sivanandam and Deepa, 2008).

## 4. Numerical experiments

### 4.1 Experimental design

We design numerical experiments by using actual data set provided by UCI machine learning repository to evaluate classification performance of classifier obtained by  $1 - HRD_d$ . 7 data set named Iris, Biomed, Liver, Breast, Vehicle, Abalone, Satellite are considered and [Table 1] summarizes the detailed information of data set such as the number of features or instances. However, these data sets do not accord with definition of OCC since they have more than one class. Therefore, we select a certain class as target class and consider the rest of classes as outlier, which is called One-Versus-All (OVA). OVA approach is general approach for committing OCC among MCC data set and useful for collecting information of important class selectively (Leng et al., 2015; Rayana, 2016). The selected target class of data set is also recorded in [Table 1].

**Table 1 Summary of datasets used for numerical experiments**

Datasets	Iris	Biomed	Liver	Breast	Vehicle	Abalone	Satellite
Number of attributes ( $q$ )	4	5	6	9	18	10	36
Target class	(Various)	Normal	Healthy	Malignant	Van	Class 1-8	Grey Soil
Total size	150	194	345	699	846	4,177	4,435
Size of target class	50	127	145	241	199	1,407	961
Size of outliers	100	67	200	458	647	2,770	3,474

An experiment for each data set was performed as follows. We randomly selected half of instances belonging to target class and used them as training set to learn proposed classifier. After classifier is formulated by using training set, the rest half of target class not used as training set and all instances defined as outliers were used as test data to verify the classifier. In Iris data set, for instance, training data set consisted of 25 instances randomly selected from target class and test data set consisted of rest 25 instances belonging to target class and 100 outliers. To set parameters of GA, pre-experiment was carried out resulting in population size  $P = 20$ , and probability of mutation  $p_m = 0.01$ .

We considered such configuration of training and target class due to measure used to evaluate classification performance of classifiers, namely AUC. AUC is representative performance measure for classifier, and it can inspect classifier in terms of both capability for including target class instances that we are interested in and excluding outliers simultaneously. Since test set considered in this paper contains instances of target class and outlier, AUC can be computed by how many instances of target class are included and how many outliers are excluded among the test set. ROC curve for calculation of AUC is drawn by of true positive rate (TPR) representing the ratio of instances classified as positive among actual positive instances and false positive rate (FPR) representing the ratio of instances classified as positive among actual negative instances. Concretely, we drew ROC curve by increasing  $v_r$  in fitting function, determining the length of intervals, until all instances of target class in test dataset are covered. [Figure 10] depicts one ROC curve and AUC value obtained by using  $1 - HRD_d$ , which was constructed by using one chromosome for Biomed dataset. Previous work proved this approach for drawing ROC curve was superior to drawing ROC curve based on other parameters (Jeong et al., 2019).

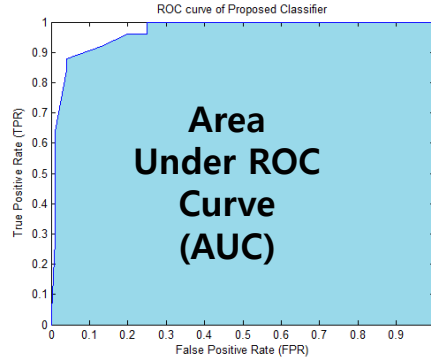


Figure 10. Example of AUC

#### 4.2 Pre-test for selection of kernel function

As we mentioned previously, kernel function  $K$  is an essential component since it influences derivation of the number of Gaussian distributions  $N_{g_r}$  used in feature  $r$ , which determines shape of resulted H-RTGL and classification performance. There exist various kernel functions to be considered in KDE, and we carried out pre-test to choose kernel function that can ensure faster convergence speed and more accurate classification result in classifier generation of  $1 - HRD_d$  with GA. Especially, we compared 4 kernel functions namely uniform kernel, triangular kernel, Gaussian kernel, cosine kernel. Brief description of each kernel function is summarized as [Table 2] including type, equation of kernel function and graphs of function. All numerical experiments as well as pre-test for selection of kernel function were implemented via MATLAB R2017b in PC platform with 16GB RAM and an Intel (R) Core (TM) i5-3570 CPU 3.40 GHz.

Table 2 Various type of kernel functions and brief description of them

Kernel type	Kernel function $K(u)$	Graphs of function
Uniform	$K(u) = \frac{1}{2}$	
Triangular	$K(u) = (1 -  u )$	
Gaussian	$K(u) = \frac{1}{\sqrt{2\pi}} e^{-\frac{1}{2}u^2}$	
Cosine	$K(u) = \frac{\pi}{4} \cos\left(\frac{\pi}{2}u\right)$	

We executed GA to generate  $1 - HRD_d$  for data set considered in this paper by using above-mentioned kernel functions. [Table 3] summarizes the average number of generations until convergence and standard deviation, which is resulted from 20 replications for each kernel function. Particularly, Virginica class is chosen as representative of Iris data set since it has the slowest convergence speed among three classes.

**Table 3 Result of pre-test for choosing kernel function**

Dataset \ Kernel type	Iris (Virginica)	Biomed	Liver	Breast	Vehicle	Abalone	Satellite
The average number of generations until convergence (Standard deviation)							
Uniform kernel	6.75 (1.43)	7.80 (1.65)	7.25 (1.05)	7.65 (1.58)	<b>11.35 (1.92)</b>	<b>13.45 (2.54)</b>	<b>17.55 (2.46)</b>
Triangular kernel	6.95 (1.52)	7.95 (1.72)	7.20 (0.98)	7.40 (1.46)	<b>10.85 (2.09)</b>	<b>12.95 (2.83)</b>	<b>18.00 (2.33)</b>
Gaussian kernel	6.90 (1.33)	7.55 (1.24)	7.10 (0.99)	7.45 (1.64)	<b>8.05 (1.42)</b>	<b>9.05 (1.52)</b>	<b>11.05 (1.88)</b>
Cosine kernel	6.80 (1.67)	7.70 (1.31)	7.15 (1.06)	7.55 (1.54)	<b>8.00 (1.35)</b>	<b>8.95 (1.44)</b>	<b>10.95 (2.01)</b>

From [Table 3], we could observe Gaussian and Cosine kernel spent less time on convergence than other kernel functions in large data set consisting of many features, namely Vehicle, Abalone, Satellite. Based on this remark, we adopted Gaussian kernel for one-dimensional clustering procedure used in  $1 - HRD_d$ . In case of elapsed time, there was no meaningful difference according to kernel function and it took approximately 10-30ms proportional to size of data set. Moreover, no significant difference on AUC representing accuracy of classifier was observed, which indicates that kernel function only influences rapidity of convergence in execution of GA to generate  $1 - HRD_d$ .

#### 4.3 Experimental results

[Table 4] displays experimental results for evaluating classification performance of  $1 - HRD_d$ . Specifically, we implemented GA to generate  $1 - HRD_d$  on data set described in [Table 1] 20 times and recorded mean and standard deviation of AUC obtained from GA to generate  $1 - HRD_d$  and other OCC algorithms. We referred previous research to obtain results of existing H-RTGL based OCC methods such as  $1 - HRD_m$ ,  $1 - HRD_p$  and committed additional experiments for data set newly considered in this paper (Jeong et al., 2019). Result of other baseline OCC methods were taken from OCC results recorded by Tax (2010). Also, three variations of  $1 - HRD_d$  resulted from different fitting functions were assessed respectively and stated as  $1 - HRD_d$  (Fit 1),  $1 - HRD_d$  (Fit 2),  $1 - HRD_d$  (Fit 3). We carried out pre-test for parameter tuning based on grid search for  $1 - HRD_m$  and  $1 - HRD_p$  and state optimal parameter configurations in each data set. In case of other representative OCC algorithms, AUC values recorded in reference were acquired from parameter exploration using `dd_tools`, which is one of toolbox provided for MATLAB. Contrary to these traditional approaches, notable merit of  $1 - HRD_d$  obtained by GA is performance of classifier can be optimized by internal exploration of solution space without pre-test for parameter tuning.

**Table 4 Comparison of AUC obtained from  $1 - HRD_d$  and other one-class classifiers**

Dataset	Iris_Setosa	Iris_Versicolor	Iris_Virginica	Biomed	Liver	Breast	Vehicle	Abalone	Satellite
Classifier	AUC x 100(%) (standard deviation)								
$1 - HRD_d$ (Fit 1)	100(0.0)	99.1(0.9)	98.7(1.0)	88.5(0.9)	61.3(1.5)	94.8(0.9)	94.4(0.4)	<b>88.9(0.5)</b>	93.5(1.1)
$1 - HRD_d$ (Fit 2)	100(0.0)	98.4(0.8)	98.1(0.8)	89.4(1.5)	59.8(1.1)	96.3(0.7)	95.4(0.9)	87.8(0.8)	91.9(1.2)
$1 - HRD_d$ (Fit 3)	100(0.0)	98.7(0.9)	97.9(0.9)	90.5(1.1)	60.3(1.2)	95.9(0.8)	94.3(1.1)	87.7(0.4)	92.3(1.6)
$1 - HRD_m$ $\delta = 2, \rho = 0.2$	100(0.0) $\delta = 2, \rho = 0.2$	98.5(0.8) $\delta = 2, \rho = 0.2$	96.1(1.1) $\delta = 9, \rho = 0.2$	89.6(1.2) $\delta = 16, \rho = 0.2$	61.6(1.6) $\delta = 8, \rho = 0.2$	95.1(1.2) $\delta = 12, \rho = 0.02$	92.7(2.2) $\delta = 16, \rho = 0.3$	86.7(0.5) $\delta = 6, \rho = 0$	91.2(1.1) $\delta = 16, \rho = 0.3$
$1 - HRD_p$ $p=2$	100(0.0) $p=2$	98.2(0.8) $p=3$	97.6(0.9) $p=1$	85.2(1.2) $p=4$	59.4(2.3) $p=6$	96.2(0.7) $p=2$	83.6(2.1) $p=7$	69.0(1.6) $p=34$	83.4(0.9) $p=8$
Gauss	100(0.0)	99.4(0.4)	97.8(0.6)	90.0(0.4)	58.6(0.5)	82.3(0.2)	<b>95.6(0.1)</b>	86.1(0.2)	91.8(0.0)
MoG	100(0.0)	98.8(0.6)	97.1(0.7)	91.2(0.9)	60.7(0.6)	78.5(1.3)	95.0(0.1)	85.3(0.5)	40.0(0.9)
Näive Parzen	100(0.0)	98.3(0.6)	95.4(1.1)	93.1(0.2)	61.4(0.7)	<b>96.5(0.4)</b>	86.9(0.2)	85.9(0.4)	<b>97.1(0.1)</b>
Parzen	100(0.0)	99.0(0.3)	96.5(0.8)	90.0(1.1)	59.0(0.3)	72.3(0.5)	47.1(8.6)	86.3(0.1)	53.5(0.0)
$k$ -means	100(0.0)	98.4(1.0)	95.4(0.5)	87.8(1.2)	57.8(1.0)	84.6(3.5)	88.9(0.6)	79.2(1.1)	88.6(18.6)
$k$ -NN	100(0.0)	98.3(0.2)	97.0(0.8)	89.1(0.8)	59.0(0.9)	69.4(0.6)	70.6(8.9)	86.5(0.1)	55.1(0.0)
SOM	100(0.0)	98.3(0.5)	96.6(0.3)	88.7(0.8)	59.6(0.7)	79.0(2.3)	84.6(0.8)	81.4(0.3)	96.4(0.2)
SVDD	100(0.0)	98.5(0.1)	98.1(0.8)	52.2(0.3)	59.0(0.9)	70.3(0.5)	0.3(0.0)	80.6(0.1)	19.5(0.0)
LPDD	100(0.0)	97.8(0.5)	98.6(0.4)	87.5(0.9)	56.4(2.6)	80.0(0.5)	38.6(9.7)	69.7(0.1)	52.8(0.0)

At first, we could observe that classification performance of variations  $1 - HRD_d$  (Fit 1) to  $1 - HRD_d$  (Fit 3) using different fitting function were different despite the same data set considered. We could also infer that superiority of fitting function varied depending on data set since there was no  $1 - HRD_d$  outperformed others in all data set. In data set such as Breast and Vehicle, for instance, the most promising approach was  $1 - HRD_d$  (Fit 2) formulates H-RTGL by using intervals without any fitting operation. This statement can be interpreted that such data set has relatively small risk of overfitting into training data set with instances evenly located in feature space. On the other hand,  $1 - HRD_d$  (Fit 3) generated the most accurate classifier in Biomed data set, which implies that the data set is organized well and fits with Gaussian distribution. As a result, proposed fitting functions enable  $1 - HRD_d$  to deal with various data set with various structures.

Classifiers obtained from GA to generate  $1 - HRD_d$  showed superior performance compared to those obtained from traditional H-RTGL based OCC methods such as  $1 - HRD_m$ ,  $1 - HRD_p$  in spite of fluctuation according to fitting function. We could observe 1-8% of difference in terms of AUC except for Liver data set, which showed nearly the same classification performances between  $1 - HRD_d$  and existing  $1 - HRD$ s. By the way, further research proved that a feature named Number of Half-pint Equivalents of Alcoholic Beverages Drunk per day included in Liver data set was not appropriate for dividing healthy and not healthy classes (Forsyth, 2009). This can explain relatively low AUC value of Liver data set and suggest that the data set is not suitable for assessing classifier due to defective feature. From the viewpoint of internal mechanism of classifier,  $1 - HRD_d$  proposed in this paper has similar aspect to  $1 - HRD_p$  generating intervals by partitioning of large interval since it divides projection points into clusters. Difference between  $1 - HRD_p$  and  $1 - HRD_d$  stems from limitation of  $1 - HRD_p$  that the same number of partitioning is applied for all features and partitioning is carried out by considering merely distance between instances, which ignores density of data set and deviation according to features. Peculiarly, performance degradation of  $1 - HRD_p$  observed in data set with many features such as Vehicle, Abalone, Satellite supports dominance of proposed  $1 - HRD_d$ .

Considering OCC algorithms other than H-RTGL based OCC, the classification performance

of  $1 - HRD_d$  obtained by GA was recorded the highest AUC value in Iris\_Setosa, Iris\_Virginica, Abalone. In addition, gap between the classification performance of  $1 - HRD_d$  obtained by GA and that of the most prominent OCC algorithm was very close, specifically 0.2-0.3%. These results indicate that  $1 - HRD_d$  has competitiveness in terms of classification performance against well-known OCC algorithms as well as existing H-RTGL based OCC methods. Meanwhile, even though Naïve Parzen and Gauss show higher classification accuracy than variations of  $1 - HRD_d$ , they are based on density estimation method which has an issue for threshold to discriminate target class. User has also difficulty on deriving remarks from their classification results due to lack of clear basis for post analysis. On the other hand,  $1 - HRD_d$  can provide interpretability proven in next subsection with maintaining considerable classification performance.

#### 4.4 Proof of Interpretability

In addition to classification performance proven as above-mentioned numerical experiments, valuable insight and clear interpretation can be achieved by  $1 - HRD_d$  since resulted classifier consists of geometric rules that can be easily understood by user. We considered Iris and Biomed data set as an example of such interpretation. Iris data set is composed of 3 classes corresponding to 3 species and it contains 4 features namely Sepal Length, Sepal Width, Petal Length, Petal Width. [Table 5] summarizes information of H-RTGL drawn by  $1 - HRD_d$  using Setosa class as target class. From this information, an unlabeled instance is classified as target class if it has (i) Sepal Length between 4.1-6.0, (ii) Sepal Width between 2.4 – 4.8, (iii) Petal Length between 1.1 – 1.9 and (iv) Petal Width under 0.8

**Table 5 Detailed information of  $DbH$  resulted from Iris\_Setosa**

Dataset	Features	$DbH^1$
Iris_Setosa	1. Sepal Length	4.1-6.0
	2. Sepal Width	2.4-4.8
	3. Petal Length	1.1-1.9
	4. Petal Width	0.0-0.8

[Figure 11] is a visualization result of H-RTGL described in [Table 5] and scatter plot of instances of whole Iris data set. Even if 3 features including 1. Sepal Length, 3. Petal Length, 4. Petal Width are displayed in [Figure 11], actual H-RTGL generation is committed by using all features. H-RTGL depicted in [Figure 11] includes all instances of Setosa class marked as \* while there is no instance of other class within it. Based on this, we can infer that obtained  $DbH^1$  is a representative pattern of Setosa class and intervals belonging to it are significant rules to separate Setosa class and outliers.

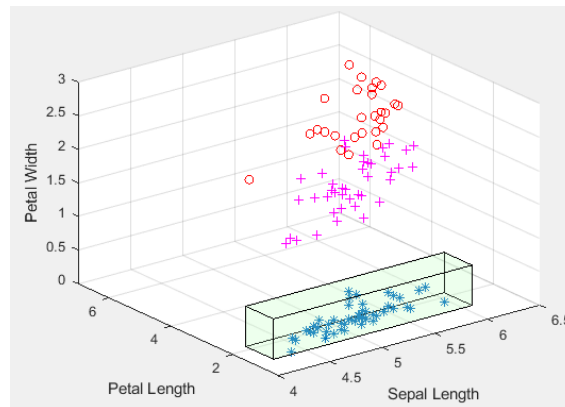


**Figure 11. Visualization of  $DbH$  resulted from Iris\_Setosa**

From the feature space described in [Figure 11], furthermore, Petal Length (y-axis) and Petal Width (z-axis) of instances belonging to Setosa class are significantly different from those considered as outlier while Sepal Length (x-axis) of instances belonging to Setosa class and other classes is not so far in feature space. User can consider Petal Length and Petal Width as important features to determine the unlabeled instance as Setosa class based on the observation.

Next, Biomed data set aims to identify factors bringing about a certain genetic disorder and it consists of five features including age of patient and values of 4 blood measurements. We generated following *DbHs* expressed as [Table 6] considering Normal class as target class. Also, [Table 7] is a confusion matrix calculated from actual classification result of test data set by using information recorded in [Table 6].

**Table 6 Detailed information of *DbHs* resulted from Biomed**

Dataset	Features	<i>DbH</i> <sup>1</sup>	<i>DbH</i> <sup>2</sup>	<i>DbH</i> <sup>3</sup>	<i>DbH</i> <sup>4</sup>
Biomed	1. Age	20-28	20-28	31-39	31-39
	2. Measure 1	18-38	18-38	40-70	40-70
	3. Measure 2	56.0-76.5	56.0-76.5	75.0-87.5	87.0-109.0
	4. Measure 3	3.9-12.0	3.9-12.0	10.7-21.6	10.7-21.6
	5. Measure 4	97-141	140-166	164-198	203-315

**Table 7 Confusion matrix for test data set of Biomed**

		Classification result by <i>DbH</i>	
		Target class	Outlier
Actual membership	Target class	56	7
	Outlier	10	57

From confusion matrix, we could observe 4 *DbHs* covered 56 instances belonging to target class among 63 instances of target class in whole test set and 10 outliers. Therefore, coverage of resulted classifier was  $56/63 = 88.8(\%)$  and classification accuracy of it was  $56/66 = 84.8(\%)$ . Such relatively high coverage and classification accuracy mean that *DbHs* comprising  $1 - HRD_d$  are representative pattern of Biomed data set and they split Normal class corresponding to target class and outliers appropriately. In terms of each feature, measure 1 of *DbHs* describing Normal class was 18-38 or 40-70 while average value of measure 1 of outlier was 185.8, which can support that measure 1 is an important feature causing the genetic disorder. As described in this subsection, such insight including the importance of certain feature can be gathered from H-RTGL generated by GA in this manner.

Lastly, Breast data describes some characteristics of a tumor in breast such as thickness, and its objective is to discriminate Benign and Malignant tumor. [Table 8] summarizes information of 3 *DbHs* covering the most instances obtained by  $1 - HRD_d$ . Also, [Table 9] is a confusion matrix calculated from actual classification result of test data set by using information recorded in [Table 8].

**Table 8 Detailed information of *DbHs* resulted from Breast**

Dataset	Features	<i>DbH</i> <sup>1</sup>	<i>DbH</i> <sup>2</sup>	<i>DbH</i> <sup>3</sup>
Breast	1. Clump thickness	3-6	6-8	9-10
	2. Uniformity of cell size	2-4	5-7	8-10
	3. Uniformity of cell shape	4-6	7-10	7-10
	4. Marginal Adhesion	1-10	1-10	1-10
	5. Single Epithelial cell size	2-4	2-4	5-6
	6. Bare Nuclei	4-6	7-10	7-10
	7. Bland Chromatin	2-3	4-5	6-7
	8. Normal Nuclei	1-5	1-5	6-10
	9. Mitoses	1-2	2-5	7-10

**Table 9 Confusion matrix for test data set of Breast**

		Classification result by <i>DbH</i>	
		Target class	Outlier
Actual membership	Target class	90	30
	Outlier	16	442

From confusion matrix, we could observe 3 *DbHs* covered 90 instances belonging to target class among 120 instances of target class in whole test set and 16 outliers. Therefore, coverage of resulted classifier was  $90/120 = 75.0(\%)$  and classification accuracy of it was  $90/106 = 84.9(\%)$ . Similar to case of Biomed, *DbHs* obtained by  $1 - HRD_d$  are typical pattern of Breast data set and they distinguish an instance of Malignant class and that belonging to outlier well. Additional interpretation of pattern by means of each feature is as follows. At first, values of Marginal adhesion recorded in 3 *DbHs* are 1-10 in common. Since Breast data is normalized between 1 to 10, that feature can hardly be regarded as an important feature discriminating Malignant class. Contrary to Marginal adhesion, values of Uniformity of cell shape and Bare Nuclei recorded in [Table 8] are relatively narrow, which implies they are essential features describing Malignant class. We explored Chen et al. (2011) to validate feature importance inferred by  $1 - HRD_d$ . They carried out correlation analysis between each feature and class information, which indicated that Uniformity of cell shape and Bare Nuclei had high correlation coefficient of 0.8219 and 0.8227. In addition, Marginal adhesion had low correlation coefficient of 0.7062. As a result, relevance of interpretation about feature importance based on  $1 - HRD_d$  is proven by cross-validation.

## 5. Conclusion

In this paper, we mainly tackled (i) development of a novel OCC classifier named  $1 - HRD_d$  considering density and distribution of training data and (ii) design of GA which enables systematic generation of the classifier with optimizing hyperparameter. Interval generation method of  $1 - HRD_d$  includes one-dimensional clustering procedure reinforced with KDE and Jenks, which can reflect latent patterns or distributions of data well. Also, we devised encoding scheme compromised of genes representing the number of normal distributions  $Ng_r$  in each feature  $r$  and other genetic operators suitable for chromosome structure to derive a promising parameter configuration. To validate performance of proposed  $1 - HRD_d$  generated by GA, we carried out numerical experiments using actual data set and provided an example of clear interpretation about resulted classifier and data set.

The experiment showed classification performance of  $1 - HRD_d$  obtained by GA was similar or superior to other OCC algorithms that can guarantee high performance but not interpretability such as SVDD or 1-SVM. In addition, the performance of  $1 - HRD_d$  obtained by GA was also dominant to previous H-RTGL based OCC methods such as  $1 - HRD_m$  or  $1 - HRD_p$ . Based on these, we can conclude  $1 - HRD_d$  obtained by GA overcome the difficulty of parameter tuning in traditional H-RTGL based OCC research as well as trade-off occurring in existing other OCC algorithms in terms of classification performance and interpretability. As a result, learning latent but important pattern of data set and interpreting resulted classifier for post analysis based on the contribution of our work. For instance, we can consider an application such as outlier detection in manufacturing field to report factor causing deflection by learning patterns of proper and defected products.

Meanwhile, there exist plenty of topics to consider as further works although we could prove effectiveness and efficiency of GA to generate  $1 - HRD_d$  in terms of i) extension to other data set, ii) modification of internal mechanism of classifier and iii) application of other metaheuristics. In addition to UCI machine learning data set considered in this paper, we plan to verify our work by using exceptionally large or complex data set including inherent problematic structure. Also, we intend to develop interval generation methods using other distributions than normal distribution since some data set is not suitable for normal distribution. Application of state-of-the-art metaheuristics such as Particle Swarm Optimization (PSO) known for faster convergence than GA is another option.

## References

- Aggarwal, C. C. (Ed.). (2014). "Data classification: algorithms and applications". CRC press.
- Bishop, C. M. (1994). "Novelty detection and neural network validation". *IEEE Proceedings-Vision, Image and Signal processing*, 141(4), 217-222.
- Brause, R., Langsdorf, T., & Hepp, M. (1999). "Neural data mining for credit card fraud detection. In Tools with Artificial Intelligence". *1999. Proceedings of 11th IEEE International Conference on* 103-106.
- Campbell, C., & Bennett, K. P. (2001). "A linear programming approach to novelty detection". *In Advances in neural information processing systems*, 395-401.
- Cohen, I., Sebe, N., Gozman, F. G., Cirelo, M. C., & Huang, T. S. (2003). "Learning Bayesian network classifiers for facial expression recognition both labeled and unlabeled data". *In Computer Vision and Pattern Recognition, 2003. Proceedings. 2003 IEEE Computer Society Conference on* 1-1.
- Datta, P. (1997). "Characteristic Concept Representations". University of California at Irvine, PhD Thesis

- De Comite, F., Denis, F., Gilleron, R., & Letouzey, F. (1999). "Positive and unlabeled examples help learning". In *International Conference on Algorithmic Learning Theory*, 219-230.
- de Ridder, D., Tax, D., & Duin, R. (1998). "An experimental comparison of one-class classification methods". In *Proceedings of the 4th Annual Conference of the Advanced School for Computing and Imaging, Delft*.
- Deep, K., & Thakur, M. (2007). "A new crossover operator for real coded genetic algorithms". *Applied mathematics and computation*, 188(1), 895-911.
- Denis, F., Gilleron, R., & Letouzey, F. (2005). "Learning from positive and unlabeled examples". *Theoretical Computer Science*, 348(1), 70-83.
- Desforges, M. J., Jacob, P. J., & Cooper, J. E. (1998). "Applications of probability density estimation to the detection of abnormal conditions in engineering". *Proceedings of the Institution of Mechanical Engineers, Part C: Journal of Mechanical Engineering Science*, 212(8), 687-703.
- Forsyth, C. B., Farhadi, A., Jakate, S. M., Tang, Y., Shaikh, M., & Keshavarzian, A., (2009), "Lactobacillus GG treatment ameliorates alcohol-induced intestinal oxidative stress, gut leakiness, and liver injury in a rat model of alcoholic steatohepatitis", *Alcohol*, 43(2), 163-172.
- Hao. (2008). "Fuzzy one-class support vector machines". *Fuzzy Sets and Systems*, 159.
- Hempstalk, K., & Frank, E. (2008). "Discriminating against new classes: One-class versus multi-class classification". In *Australasian Joint Conference on Artificial Intelligence*. 325-336.
- Hempstalk, K., Frank, E., & Witten, I. H. (2008). "One-class classification by combining density and class probability estimation". In *Joint European Conference on Machine Learning and Knowledge Discovery in Databases* 505-519.
- Jeong, I. K., & Choi, J. Y., (2015), "Design of one-class classifier using hyper-rectangles", *Journal of the Korean Institute of Industrial Engineers*, 41(5), 439-446.
- Jeong, I. K., Kim, D. G., Choi, J. Y., & Ko, J. (2019). "Geometric one-class classifiers using hyper-rectangles for knowledge extraction". *Expert Systems with Applications*, 117, 112-124.
- Kang, S., Cho, S., & Kang, P. (2015). "Multi-class classification via heterogeneous ensemble of one-class classifiers". *Engineering Applications of Artificial Intelligence*, 43, 35-43.
- Kim, D. G., Choi, J. Y., & Ko, J. (2018). "An Efficient One Class Classifier Using Gaussian-based Hyper-Rectangle Generation". *Journal of Society of Korea Industrial and Systems Engineering*, 41(2), 56-64.
- Le, T., Tran, D., Ma, W., & Sharma, D. (2010). "An optimal sphere and two large margins approach for novelty detection". In *Neural Networks (IJCNN), The 2010 International Joint Conference on*, 1-6.
- Le, T., Tran, D., Ma, W., & Sharma, D. (2011). "Multiple distribution data description learning algorithm for novelty detection". In *Pacific-Asia Conference on Knowledge Discovery and Data Mining* 246-257.
- Lee, W., Stolfo, S. J., & Mok, K. W. (1999). "A data mining framework for building intrusion detection models". *Proceedings of the 1999 IEEE Symposium in Security and Privacy*, 120-132.
- Liu, Y., & Madden, M. G. (2007). "One-class support vector machine calibration using particle swarm optimisation".
- Makinen, R. A., Periaux, J., & Toivanen, J. (1999). "Multidisciplinary shape optimization in

aerodynamics and electromagnetics using genetic algorithms”. *International Journal for Numerical Methods in Fluids*, 30(2), 149-159.

Moya, M. M., & Hush, D. R. (1996). “Network constraints and multi-objective optimization for one-class classification”. *Neural Networks*, 9(3), 463-474.

Pimentel, M. A., Clifton, D. A., Clifton, L., & Tarassenko, L. (2014). “A review of novelty detection”. *Signal Processing*, 99, 215-249.

Scholkopf, B., Williamson, R., Smola, A., Taylor, J.S. & Platt, J., (2000), “Support vector method for novelty detection”, *Advances in Neural Information Processing Systems*, 12, 582-588.

Silverman, B.W. (1986). “Density Estimation for Statistics and Data Analysis”. London: Chapman & Hall/CRC.

Sivanandam, S. N., & Deepa, S. N. (2008). “Genetic algorithm optimization problems”. *In Introduction to Genetic Algorithms*, 165-209.

Sun, Y., Wong, A. K., & Kamel, M. S. (2009). “Classification of imbalanced data: A review”. *International Journal of Pattern Recognition and Artificial Intelligence*, 23(4), 687-719.

Tandon, G., & Chan, P. K. (2007). “Weighting versus pruning in rule validation for detecting network and host anomalies”. *In Proceedings of the 13th ACM SIGKDD international conference on Knowledge discovery and data mining*, 697-706.

Tax, D. M., & Duin, R. P. (1999). “Support vector domain description”. *Pattern recognition letters*, 20(11-13), 1191-1199.

Tax, D. M., & Duin, R. P. (2004). “Support vector data description”. *Machine learning*, 54(1), 45-66.

Tax, D.M., (2010), “One-class classifier results”, URL <http://homepage.tudelft.nl/n9d04/occ/>

Tian, J., & Gu, H. (2010). "Anomaly detection combining one-class SVMs and particle swarm optimization algorithms". *Nonlinear Dynamics*, 61(1-2), 303-310.

Xiao, Y., Liu, B., Cao, L., Wu, X., Zhang, C., Hao, Z., & Cao, J. (2009). “Multi-sphere support vector data description for outliers detection on multi-distribution data”. *In ICDMW'09. IEEE International Conference on Data Mining Workshops*, 82-87.

Yu, H. (2005). “Single-class classification with mapping convergence”. *Machine Learning*, 61(1-3), 49-69.